

# Ecosystem engineering by periphyton in Alpine proglacial streams

Matteo Roncoroni<sup>1</sup>  | Aurélien Ballu<sup>1</sup> | Adrijan Selitaj<sup>1</sup> | Davide Mancini<sup>1</sup> | Floreana Miesen<sup>1</sup> | Marc Aguet<sup>1</sup> | Tom I. Battin<sup>2</sup> | Stuart N. Lane<sup>1</sup> 

<sup>1</sup>Institute of Earth Surface Dynamics, University of Lausanne, UNIL Mouline, Lausanne, Switzerland

<sup>2</sup>River Ecosystems Laboratory, Alpine and Polar Environmental Research Center Ecole Polytechnique Fédérale de Lausanne (EPFL), Lausanne, Switzerland

## Correspondence

Matteo Roncoroni, Institute of Earth Surface Dynamics, University of Lausanne, UNIL Mouline, Lausanne, Switzerland.  
Email: [matteo.roncoroni@unil.ch](mailto:matteo.roncoroni@unil.ch)

## Funding information

Swiss National Science Foundation Sinergia, Grant/Award Number: CRSII5\_180241

## Abstract

Stream periphytons are candidate ecosystem engineers in proglacial margins. Here, we quantify the extent to which they are engineers for the case of hillslope-fed tributaries in the terrace zones of proglacial margin alluvial plains. Candidate ecosystem engineering effects relate to periphyton-driven changes in (1) vertical infiltration of water, which in turn could aid plant colonization and hence local surface stabilization, and (2) near-bed hydraulics, notably near-bed turbulence properties. We ran two flume experiments in parallel in the proglacial margin of the Otemma glacier (Switzerland), reproducing the environmental conditions found in terrace streams. In both experiments, we followed periphyton development on initially bare sediments for 28 days. Then, whilst the experiment continued undisturbed in one flume, in the second and over a further 26 days, we introduced disturbances in the form of desiccation events. Throughout the entire experiment length, we collected imagery for close-range SfM-MVS photogrammetry, data on vertical infiltration, and near-bed hydraulics. The experiments showed that periphyton development significantly changed the streambed properties. First, periphyton development over the timescale of a few days reduced bed roughness and clogged the benthic interstitial space, reducing water infiltration. These effects were insensitive to the disturbance regime. Second, the changes in streambed roughness modified the near-bed turbulent structures, and this resulted in a reduction of bursting events and in the modification of the turbulent kinetic energy at the near-bed layer. The latter, however, appeared to be less important in these environments as compared with the impacts on infiltration. Given the low water retaining capacity of glacial sediments, the observation that periphyton can reduce vertical infiltration explains wider observations of their importance in glacial floodplains where vegetation succession is critically constrained by water availability. The relatively reduced impacts on near-bed turbulence also contribute to explaining why disturbance in proglacial margin streams remains a key limit on ecological succession.

## KEYWORDS

ecosystem engineering, glacial floodplains, infiltration, near-bed turbulence, periphyton, proglacial streams

This is an open access article under the terms of the [Creative Commons Attribution](https://creativecommons.org/licenses/by/4.0/) License, which permits use, distribution and reproduction in any medium, provided the original work is properly cited.

© 2023 The Authors. *Earth Surface Processes and Landforms* published by John Wiley & Sons Ltd.

## 1 | INTRODUCTION

Stream periphytons are implicated in multiple ecosystem processes such as carbon fluxes and nutrient uptake/recycling (Battin et al., 2016; Battin, Kaplan, Denis Newbold, & Hansen, 2003). Recently, they have been included as ecosystem engineers (Gerbersdorf, Manz, & Paterson, 2008; Gerbersdorf et al., 2009; Roncoroni et al., 2019). Periphytons are thought to have three broad potential engineering impacts. First, they may stabilize sediments by increasing the critical bed shear stress  $T_{oc}$  required for sediment movement (Fang et al., 2014; Gerbersdorf, Jancke, et al., 2008; Gerbersdorf et al., 2009; Le Hir et al., 2007; Neumeier et al., 2006; Pivato et al., 2019; Thom et al., 2015; Vignaga et al., 2013). The secretion of extracellular polymeric substances (EPS) leads to physical binding of and/or molecular electrochemical interactions between substrate grains (Dade et al., 1990; Grant & Gust, 1987; Tolhurst et al., 2002). This effect appears to be particle-size dependent, more effective for finer grains (Statzner et al., 1999) and a function of both seasonality (Amos et al., 2004; Pivato et al., 2019; Schmidt et al., 2016; Thom et al., 2015; Widdows et al., 2000), and periphyton growth history (Mariotti & Fagherazzi, 2012).

Second, periphytons may modify near bed hydrodynamics through their effects on the micromorphology of the river bed surface (Fang et al., 2014; Kazemifar et al., 2021; Nikora et al., 1997, 2002). Periphyton development may decrease (Labioud et al., 2007) or increase (Nikora et al., 1997; Piqué et al., 2016) bed roughness, but also decrease porosity by filling particle pores (Kazemifar et al., 2021). Such phenomena could ultimately dampen, in the case of reduced roughness and porosity, or enhance, in the case of increased roughness, near-bed Reynolds shear stresses (Breugem et al., 2006; Kazemifar et al., 2021; Suga et al., 2010). Decomposition of the Reynolds shear stress into turbulence quadrants (i.e., outward interactions, ejections, inward interactions, and sweeps) (Nelson et al., 1995) may be important because bursting processes, and particularly sweep and ejection events, play an active role in sediment entrainment and transport (Bennett & Best, 1995; Dwivedi et al., 2011; Keylock et al., 2014; Mianaei & Keshavarzi, 2010; Paiement-Paradis et al., 2011; Thorne et al., 1989; Wu & Jiang, 2007). Periphyton development may either attenuate or enhance such processes and so impact particle movement and river-bed stability.

Changes in critical bed shear stress and turbulence intensity may impact biostabilization. It appears that biostabilization is more efficient in marine/tidal environments (Flemming & Wingender, 2010; Gerbersdorf & Wieprecht, 2015; Spears et al., 2008). This is partly due to the chemistry of seawater, which aids cohesive processes but also due to finer sediment. Biostabilization has been documented in rivers (Schmidt et al., 2016; Thom et al., 2015), but the coarser sediment composition may limit periphyton contributions. To date, it has not been investigated extensively in proglacial margin streams.

The third engineering impact may occur in parallel to biostabilization. By binding particles with EPS and filling particle pores, periphyton may clog streambed interstices (Battin & Sengschmitt, 1999; Gette-Bouvarot et al., 2014). Bed clogging reduces hyporheic exchanges between the sediment surface and sub-surface interface (Ibisch & Borchardt, 2002). The result is reduced vertical hydraulic conductivity of the sediments and hence reduced vertical water infiltration (Caruso et al., 2017; Cunningham

et al., 1991; Gette-Bouvarot et al., 2014; Ragusa et al., 1994; Thullner et al., 2002). This process may be particularly important in proglacial margins as glacial sediments are commonly well drained (Burga et al., 2010; Cooper, 1923; Matthews, 1992; Viles, 2012). Recent work (Miller & Lane, 2019; Roncoroni et al., 2019) has argued that periphyton may trigger a positive feedback in which their development promotes surface water retention so that pioneer vegetation can have a benefit.

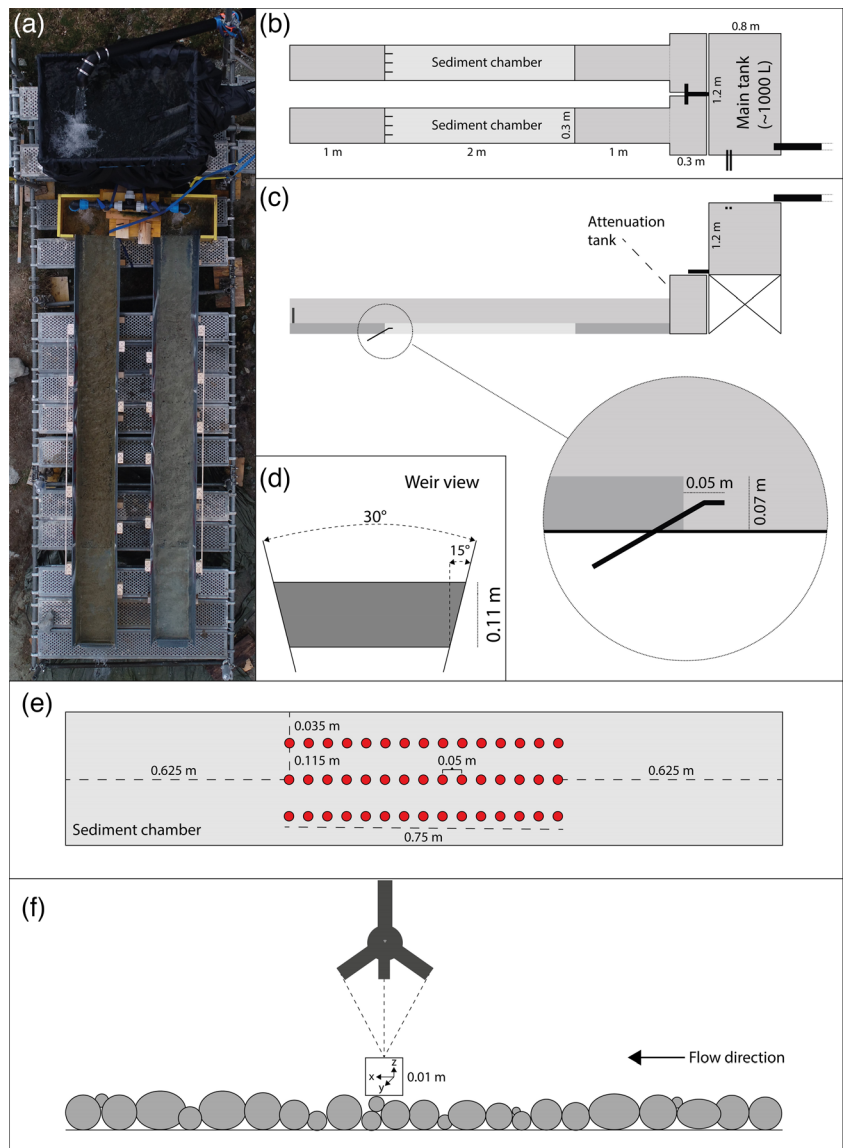
As yet, there are no quantitative studies on the combined effects of periphyton development on biostabilization and infiltration in proglacial margins, despite reviews that suggest its potential importance (Miller & Lane, 2019; Roncoroni et al., 2019). We fill this gap by running a set of outdoor flume experiments that reproduce the conditions found in stable proglacial margins where biofilms can develop (Roncoroni et al., 2023). We test the following hypotheses. First, the streambed surficial morphology evolves in response to periphyton development. Grains are rapidly coated by biomass, the benthic interstices filled, and the bed roughness reduced (H1a). If disturbances are introduced, we hypothesize that the bed tends to return to a precolonized situation, thus rougher (H1b). Second, the changes in bed roughness modify the turbulent structures in the near-bed layer, and the bursting events and the turbulent kinetic energy are likely reduced (H2a). The introduction of disturbances should change the near-bed hydraulics, as a response to the changes in bed roughness (H2b). Third, by filling streambed interstices, periphyton development reduces water vertical infiltration so that more water can be maintained more readily at the surface (H3a). However, we hypothesize that when disturbances are introduced, the periphyton effect on infiltration is partly cancelled (H3b) and this is due to the changes in bed morphology induced by the dry conditions.

## 2 | METHODS

### 2.1 | Flume and experiment setups

In order to consider periphyton development in the geographical setting of a natural proglacial margin, we installed two parallel flumes (Figure 1a, FA and FB) in the vicinity of the forefield of the Otemma Glacier (45°56'04.9"N 7°24'46.1"E). We designed the flumes to mimic the hydraulic and environmental conditions of the tributaries found on the Otemma floodplain (Roncoroni et al., 2023). In the experiments, we wanted to reproduce conditions of water transparency, hydrological and thermal stability, depth, grain-size, natural lighting, and slope. For the first part of the experiment, both flumes were run with identical conditions to assess reproducibility. They diverged for the second part of the experiment when disturbances were introduced into FA. Such disturbances were in the form of drying events that are recognized as being the primary disturbance type occurring in terrace channels during the glacial melt-season (Roncoroni et al., 2023). The experiment lasted in full for 54 days from July 14 (JD195) to September 6 (JD249) 2021. In experiment FA after 28 days of constant discharge, we introduced disturbances comprising the following: (1) a single day of dry conditions, followed by 2 days of submergence; (2) 2 days of dry conditions, followed by 3 days of submergence; (3) 3 days of dry conditions, followed by 6 days of submergence; and (4) 7 days of dry conditions, followed by 2 days of

**FIGURE 1** Flume experiment setup. (a) Aerial image of the flume setup; (b) top-view; (c) lateral view, and zoom of the buried aluminium pipes; (d) weir view; (e) ADV sampling locations; (f) ADV measurement domain.



submergence. The duration of disturbances attempted to reproduce the findings of Roncoroni et al. (2023). In experiment FB, no disturbance was introduced.

The flume structure and components were built in the field. We connected a tank (~1000 L) to a hillslope tributary and filled this tank solely by gravity. The tank had two security pipes (Figure 1b,c) intended to allow excess water to leave the tank at a given elevation above the flumes and therefore maintain a constant hydraulic head through time. At the bottom of the tank we connected a T-shape pipe with two adjustable valves (one per flume; Figure 1a-c). The water was discharged into two attenuation tanks (Figure 1c), which reduced water turbulence at the flume entrances. Water entered two trapezoidal flumes made of polyvinyl chloride (PVC) and sustained by wooded supports and a metal scaffold. Additionally, each flume exterior was equipped with 10 wooden ground control points (GCPs) (Figure 1a) for photogrammetric purposes.

The flumes were 4 m long and 0.3 m wide at the bottom (Figure 1b,c). Longitudinally in each flume there were three sections. The first was 1 m long and aimed to allow for flow adaptation to the channels. The second was 2 m long and had a PVC base that was 7 cm lower than the first section to create a sediment chamber. We packed the bed of each chamber with clean sediment sieved at 0.8–

1.6 cm (following Wolman pebble counts performed on terrace surfaces) to a thickness of 7 cm. At the end of each chamber, three buried aluminium pipes ( $\varnothing$  7 mm) collected water after vertical infiltration through the sediments for measuring the evolution in infiltration. These pipes had 1-mm mesh covers to prevent infiltration of sediment that could clog the pipes. The pipes were checked at the end of the experiment, and no sedimentation was found. The third section was 1 m long and intended to avoid flow recirculation over the sediments due to the weirs at the downstream end of each flume (Figure 1d). The weir allowed water depth to be constant at ~11.5 cm through time in each flume. The chosen depth attempted to approximate the different depths found in the tributary channels. The discharge in each flume was ~2 L/s. The overall slope of the flumes was set to 0°. An overview of the experiment initial conditions is presented in Table 1. The resultant flow depth and negligible slope was typical of the tributary-draining terrace channels in this environment.

## 2.2 | Modification of the flume beds

We produced a photogrammetric dataset of the flumes at the experiment timescale with the aim of understanding both the response of

**TABLE 1** Initial experiment conditions for both FA and FB.

Flow rate (L/s)	~2
Horizontal mean velocity (m/s)	0.05
Mean depth (m)	0.115
Bottom width (m)	0.3
Slope (°)	0
Reynolds number Re	4056.5
Froude number Fr	0.045
Grainsize range (cm)	0.8–1.6

the bed to periphyton development (H1a) and the morphological response after the introduction of disturbances (H1b). To do so, we collected daily images of the flumes with a DSLR Sony Alpha 7 III camera equipped with a Sigma Art 50-mm F1.8 lens. In addition, we measured the absolute position of 20 GCPs (10 per flume; see Figure 1a) with a differential GPS Trimble R10. The GCPs allowed orientation of the photogrammetric products into a real world coordinate system (i.e., CH1903 LV03) and reduced systematic deformations in DEMs (Butler et al., 2002; Chandler et al., 2001; James et al., 2017, 2020; Leduc et al., 2019). The images were processed in Agisoft Metashape (v. 1.5.5) through rigorous Structure-from-Motion Multi-View-Stereo (SfM-MVS) photogrammetry (James et al., 2017, 2020; James & Robson, 2014; Westoby et al., 2012). For the purposes of this study, we generated digital elevation models (DEMs) at spatial resolutions of 0.0005 m.

We evaluated the quality of FA and FB DEMs with a set of independent checkpoints ( $n = 200$  per DEM) and with respect to a relevant reference DEM (JD196, for both flumes). The error analysis revealed the presence of low-magnitude systematic deformations in the form of doming (see James & Robson, 2014) that were modelled and removed following Bakker and Lane (2017) and Mancini and Lane (2020). We also corrected our DEMs for the effect of refraction at the air-water interface (Fryer & Kniest, 1985; Westaway et al., 2000, 2001) by means of a bathymetric correction following Westaway et al. (2000, 2001). We then re-evaluated the quality of our corrected DEMs and discarded those that still had abnormally high mean errors and/or standard deviations of errors after both corrections. We therefore discarded five DEMs for FA (JD204, JD209, JD215, JD218, and JD231) and 10 for FB (JD199, JD204, JD206, JD207, JD215, JD220, JD223, JD232, JD233, and JD238) and omitted their use in further analysis to increase the robustness of our results. The retained DEMs (33 for FA; 29 for FB) were finally detrended to remove planar bedforms using a linear polynomial surface fit (Bertin et al., 2017). A detailed explanation of the photogrammetric processing and post-processing is provided in Supporting Information S1.

We then estimated the bed roughness by calculating the standard deviation of bed elevations (Aberle & Smart, 2003; Smart et al., 2004). To do so, we used a moving window of 100 pixels (i.e., 0.0025 m<sup>2</sup>) that was designed to be about two to four times the mean grain diameter and to pick up changes in surface roughness at the scale of small grain clusters. For each DEM (i.e., date), we then averaged the windowed standard deviations to obtain the mean roughness at the sediment chamber scale. Finally, we investigated the filling of benthic interstices by quantifying the elevation lows, considering the 90th percentile and the 85th and 95th percentile range of DEMs.

## 2.3 | Hydraulic data collection, processing and analysis

We investigated the evolution of the near-bed 3D flow velocities of FA and FB with the aim of understanding both how the biotic modification of the bed altered the near-bed turbulent structures (H2a) and how these are then modified by the introduction of disturbances (H2b). For this purpose, we tracked the hydraulics of FA for 12 dates (from JD197 to JD238), and FB for 13 dates (from JD197 to JD245). We collected the 3D flow velocities with an Acoustic Doppler Velocimeter (ADV), the Nortek Vectrino (VCN9421), supported by a sliding aluminium structure that allowed us to relocate the ADV precisely within the flumes. We sampled the 3D velocities of 45 points (Figure 1e), and we did this for the near-bed layer at 1 cm from the flume bottom (Figure 1f). The sampling points were divided in three parallel lines (15 points each), located at the centre of the sediment chamber and sufficiently away from the flume walls to avoid wall hydraulic interference (Figure 1e). The number of sampling locations aimed to capture most of the spatial variability in 3D velocities due to periphyton morphology. Each sampling point was measured for 60 s at a sampling rate of 25 Hz, and the sampling of each flume took in full approximately 70 to 80 min to be completed. During this time-frame, the hydraulic head was constantly monitored to avoid changes in discharge and hence in temporal modifications of the 3D velocities collected with the ADV. The data were stored in .dat format and subsequently treated and analysed in Matlab (R2021b).

The raw 3D velocities were analysed for possible noise in our time-series that could have led to inflated estimates of turbulence parameters (Cea et al., 2007; Nikora & Goring, 1998). Visual observation suggested the presence of occasional spikes, which were subsequently removed by applying the methods of Goring and Nikora (2002) and Cea et al. (2007). As we were interested in quantifying turbulent kinetic energy and the turbulent Reynolds stress tensor, we did not interpolate the missing values or replaced them with zeros (following Cea et al., 2007). Once spikes were removed, we estimated how noise was propagated into both variance (i.e.,  $\overline{uv}$ ,  $\overline{uw}$ , and  $\overline{vw}$ ) and covariance (i.e.,  $\overline{u^2}$ ,  $\overline{v^2}$ , and  $\overline{w^2}$ ) estimates following Thomas et al. (2017). This step was necessary as the variance estimates were used to calculate the total turbulent kinetic energy and the variance and covariance estimates to calculate the turbulent Reynolds stress tensor. A detailed explanation of noise removal from our time-series is provided in Supporting Information S2.

Subsequently, we extracted the Reynolds stress tensor, determined the turbulent kinetic energy, and undertook a quadrant analysis from each ADV time-series. The Reynolds stress tensor was defined as

$$\rho \begin{pmatrix} \overline{u^2} & \overline{u'v'} & \overline{u'w'} \\ \overline{v'v'} & \overline{v'w'} & \\ \overline{w'w'} & & \end{pmatrix} \quad (1)$$

We defined  $w'$  by taking the average of the two vertical components  $w$ , then removing the mean to get  $w'$ . The turbulent kinetic energy,  $k$ , was defined as

$$k = \frac{1}{2} (\overline{u^2} + \overline{v^2} + \overline{w^2}) \quad (2)$$

We finally undertook a quadrant analysis aimed at characterizing the evolution of the bursting processes in response to periphyton development. Here, the focus was given to ejection and sweep events, defined as

$$\begin{aligned} \text{Ejections } [v'_h < 0] \cap [w' > 0] \cap [|v'_h w'| > H\sigma_{v_h}\sigma_w] \\ \text{Sweeps } [v'_h > 0] \cap [w' < 0] \cap [|v'_h w'| > H\sigma_{v_h}\sigma_w] \end{aligned} \quad (3)$$

where  $v_h$  is the horizontal velocity and  $H$  is the multiplier used to define significant events, taken here as 1 (Nezu & Nakagawa, 1993). For our flume conditions, we determined a single component of horizontal velocity from  $(u^2 + v^2)^{0.5}$ , calculated  $v'_h$  from  $v_h - \bar{v}_h$ , and omitted to consider the two horizontal components of velocity ( $u$  and  $v$ ) separately in an octant analysis (e.g., Keylock et al., 2014).

As the focus of our work was to quantify the long-term-evolution ecosystem engineering impacts of periphyton development, we present these data in the same way as the streambed evolution experiments, focusing on their evolution through time at the scale of the experimental channels rather than the within-channel spatial patterns.

## 2.4 | Infiltration measurements

We investigated the modification in water vertical infiltration following periphyton development (H3a) and in response to disturbances (H3b) by collecting the water flowing out of the flumes from the buried aluminium pipes (Figure 1c). We measured the volume of water every day at 8:00 am for FA (except when the flume was dry), and at 8:15 am for FB. For both flumes, we recorded the time to fill a 500-mL bottle, weighed the content with a high precision scale, and repeated the procedure 10 times to reduce measuring bias. The daily infiltration rate was obtained by averaging the 10 measures.

## 2.5 | Statistical testing

We performed statistical testing to check for significant results. We checked for normal distributions in our data at an Alpha level of 0.05 by means of the Shapiro-Wilk test. The test reported both normal and non-normal distributions (Supporting Information S3), and therefore we made use of nonparametric tests to avoid violating test assumptions and being consistent within our analysis.

We compared our results in two ways. First, we checked for significant differences in our results by means of the Kruskal-Wallis test. We divided the results into two groups (i.e., before and after the introduction of disturbances) and analysed the median values (for roughness, ejection and sweep events, and TKE), the 90th percentiles (for the elevation lows), or the mean values (for the infiltration). This had the objectives of (i) providing meaningful information on experiment replicability before the introduction of disturbances and (ii) finding significant differences after the introduction of disturbances (i.e., significant impacts).

Second, we tested for significant monotonic increases/decreases or conversely phases without an upward or downward trend in the parameters being analysed during the experiments by means of the Mann-Kendall test, and we did this per groups (i.e., before and after the introduction of disturbances in FA) and per parameter at the

experiment timescale (i.e., from the beginning to the end of the experiment). As per the Kruskal-Wallis test, we analysed either the median values (for roughness, ejection and sweep events, and TKE), the 90th percentiles (for the elevation lows), or the mean values (for the infiltration). In both the Kruskal-Wallis and Mann-Kendall tests, the significance of the results was defined by an alpha value of 0.05.

## 3 | RESULTS

### 3.1 | Modification of the streambed

Periphyton rapidly developed and covered the streambed of FA and FB (Figures 2 and 3). As we hypothesized (H1a), the median roughness lengths (Figures 2a and 3a) significantly (Mann-Kendall:  $p < 0.05$ ) decreased by  $\sim 79\%$  in FA (JD196:  $\pm\sigma = 0.014$  m; JD223:  $\pm\sigma = 0.003$  m) and by  $\sim 71\%$  in FB (D196:  $\pm\sigma = 0.017$  m; JD222:  $\pm\sigma = 0.005$  m) between the beginning of the experiment (JD195) and the introduction of disturbances (i.e., JD224). In both cases, we noted that the median roughness lengths substantially decreased until JD210. During this first part of the experiment, both flumes did not show significant differences in the median roughness lengths (Kruskal-Wallis:  $p > 0.05$ ), suggesting similar evolutions in bed roughness.

We did not find a significant (Mann-Kendall:  $p > 0.05$ ) increase in the 90th percentile of the elevation lows in FA and FB between JD195 and JD223, although visual inspection of our results suggested that in the first 5 to 6 days the interstices were filled by biomass (Figures 2b and 3b). In statistical terms, these results were therefore in partial disagreement with our hypothesis (H1a). After this initial phase of bed modification and until the introduction of disturbances (i.e., JD224), the elevation lows somehow fluctuated, and this might have explained the absence of a significant trend. Furthermore, we could not exclude differential noise in our data, which again might have explained the absence of a significant trend. As per the roughness lengths, during this first phase (i.e., before the disturbances) the elevation lows in FA and FB did not differ significantly (Kruskal-Wallis:  $p > 0.05$ ), suggesting similar evolutions in the way periphyton covered the flume beds.

In disagreement with what we hypothesized (H1b), the roughness lengths of FA after the introduction of disturbances remained at a quasi-steady value ( $\sigma_{\text{mean}} = 0.003$ ,  $\pm\sigma = 0$  m) without any significant upward trend (Mann-Kendall:  $p > 0.05$ ). There were two outliers to this quasi-steady state, JD238 ( $\pm\sigma = 0.009$  m) and JD239 ( $\pm\sigma = 0.006$  m), which had greater median roughness lengths. These exceptions might be related to localized detachments of periphyton (see the upstream part of FA at JD239; Figure 2d), or to fluctuations of the periphyton mat at the time of image acquisition. We cannot exclude differences in DEM noise. The quasi-steady pattern of FA was similar in FB (Figure 3a;  $\sigma_{\text{mean}} = 0.003$ ,  $\pm\sigma = 0$  m), although our results suggested that FB experienced low magnitude fluctuations in bed roughness, and these likely related to the detachment of localized periphyton patches and the formation of holes on the periphyton carpet from JD224 onwards (Figure 5d). During the second part of the experiment, we did not find significant differences in the median roughness lengths of FA and FB (Kruskal-Wallis:  $p > 0.05$ ), suggesting that the introduction of disturbances had little influence on the roughness lengths of FA.

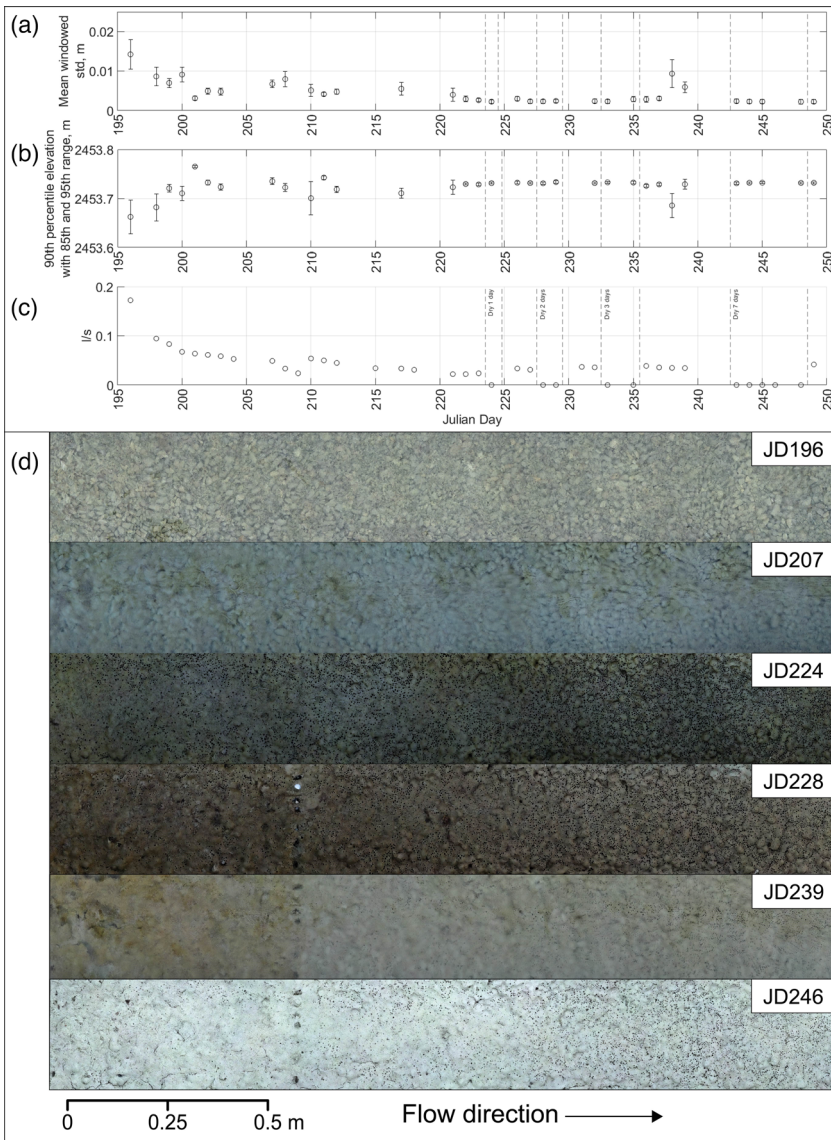


**FIGURE 2** Streambed evolution of FA. (a) Streambed roughness, expressed as the mean windowed standard deviations of the streambed elevations (m). (b) Interstice filling, expressed as the elevations lows (m), presenting the 90th percentile and the 85th and 95th percentile range (where the percentile is counted from high to low elevations). (c) Infiltration (L/s) evolution through time; (d) visual appreciation of the evolution of the streambed.

In this second phase, the 90th percentiles of the elevation lows of FA (Figure 2b) were quasi-steady at  $\sim 2453.73$  m ( $\pm\sigma = 0.002$  m), and no significant downward trend was noted (Mann–Kendall:  $p > 0.05$ ) suggesting biomass removal was not detected. As per the roughness lengths, this result disagreed with our initial hypothesis (H1b). There was an exception; JD238 (90th percentile = 2453.69 m) experienced a drop that might be explained by some localized detachments or by the fluctuations of the periphyton mat. As per FA, the interstices of FB (Figure 3b) experienced a phase of quasi-steadiness and remained at a level of  $\sim 2453.76$  m ( $\pm\sigma = 0.001$  m). Although the elevation lows were quasi-steady in both flumes, we found significant differences (Kruskal–Wallis:  $p < 0.05$ ) in the 90th percentile of the lows of FA and FB, suggesting the potential impact of the disturbances, differences in periphyton morphology, or because of differential noise.

In summary, at the experiment timescale (i.e., from the beginning to the end of the experiment), our results suggested the following patterns. The median roughness lengths decreased significantly (Mann–Kendall:  $p < 0.05$ ) in both flumes; by  $\sim 86\%$  in FA (JD196:  $\pm\sigma = 0.014$  m; JD249:  $\pm\sigma = 0.002$  m) and by  $\sim 82\%$  in FB (JD196:  $\pm\sigma = 0.017$  m; JD249:  $\pm\sigma = 0.003$  m). The 90th percentile of the elevation lows increased significantly (Mann–Kendall:  $p < 0.05$ ) in both flumes; by  $\sim 0.003\%$  in FA (JD216: 2453.66 m,  $\pm\sigma = 0.03$  m; JD249:

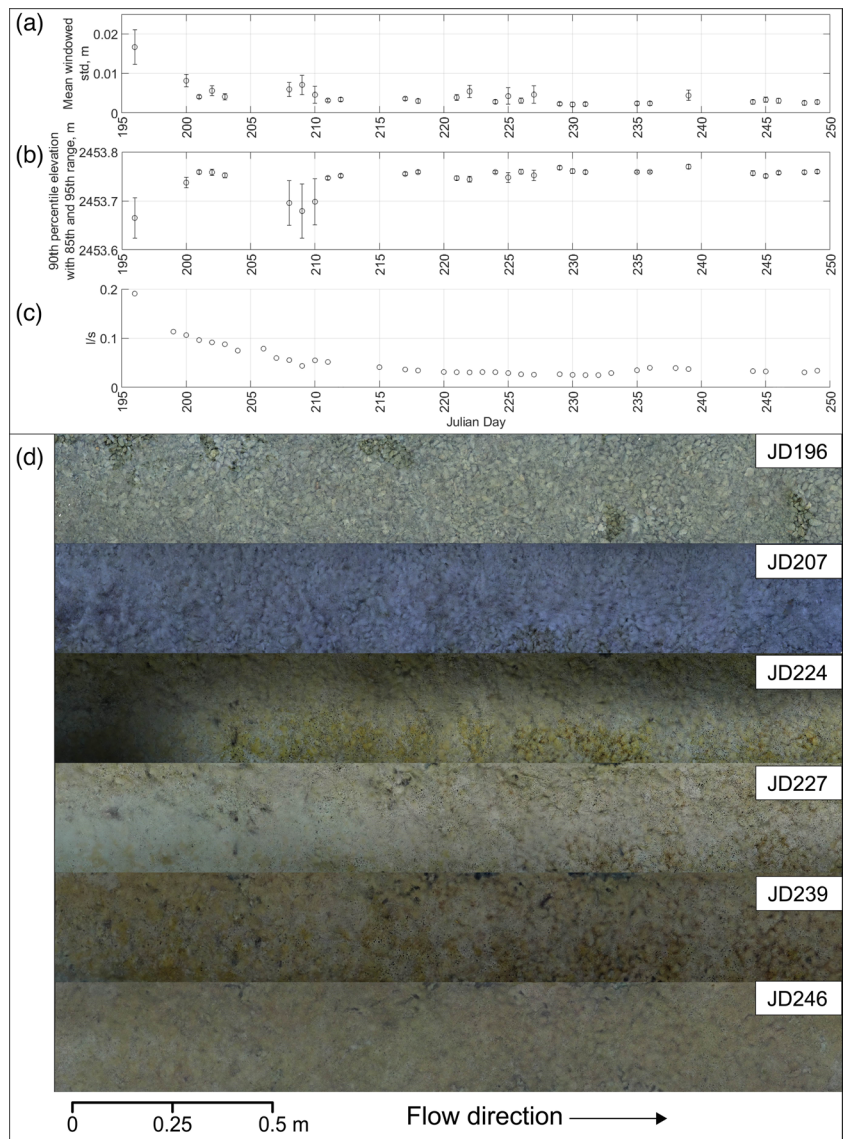
2453.73 m,  $\pm\sigma = 0.002$  m) and by  $\sim 0.004\%$  in FB (JD216: 2453.66 m,  $\pm\sigma = 0.04$  m; JD249: 2453.7598 m,  $\pm\sigma = 0.004$  m). These results further highlighted the disagreement with our initial hypothesis (H1b), illustrating that the bed of FA did not return to a precolonization level.

### 3.2 | Infiltration rates

As hypothesized (H3a), the infiltration rate was reduced in both flumes (Figures 2c and 3c) between the beginning of the experiment and JD223. In FA, the infiltration was significantly (Mann–Kendall:  $p < 0.05$ ) reduced by  $\sim 88\%$  between JD196 (0.17 L/s) and JD223 (0.02 L/s). Similarly, the rate in FB was reduced by  $\sim 84\%$  between JD196 (0.19 L/s) and JD223 (0.03 L/s), and this reduction was also found to be significant (Mann–Kendall:  $p < 0.05$ ). During this first part of the experiments, the evolution in infiltration of FA and FB did not significantly differ (Kruskal–Wallis:  $p > 0.05$ ), suggesting a co-evolution in the way the infiltration was reduced in both flumes.

In disagreement with our hypothesis (H3b), the infiltration in FA did not return to a precolonized level (no significant upward trend detected; Mann–Kendall:  $p > 0.05$ ), and appeared to remain

**FIGURE 3** Streambed evolution of FB. (a) Streambed roughness, expressed as the mean windowed standard deviations of the streambed elevations (m). (b) Interstice filling, expressed as the elevations lows (m), presenting the 90th percentile and the 85th and 95th percentile range (where the percentile is counted from high to low elevations). (c) Infiltration (L/s) evolution through time; (d) visual appreciation of the evolution of the streambed.



quasi-steady after the introduction of disturbances ( $\text{mean}_{\text{infiltration}} = 0.04 \text{ L/s}$ ,  $\pm\sigma = 0 \text{ L/s}$ ). However, our results suggested that disturbances might have had a slight impact on the infiltration rate (Figure 2c). In fact, we noted that after 1 day of dry conditions (JD225, 0.03 L/s), the infiltration increased by  $\sim 50\%$  compared to JD223 (0.02 L/s), although it still remained  $\sim 82\%$  less than the beginning of the experiment. Similarly, after 2 days of dry conditions (JD231, 0.4 L/s), the infiltration increased by  $\sim 33\%$  as compared to JD227 (0.03 L/s), but was still  $\sim 76\%$  less as compared to JD196 (0.17 L/s). After 3 days of dry conditions (JD236, 0.03 L/s), the infiltration did not experience any increase as compared to JD232 (0.03 L/s), while it increased by  $\sim 33\%$  between JD239 (0.03 L/s) and JD249 (0.04 L/s). Within this same period, the infiltration rate of FB was also quasi-steady ( $\text{mean}_{\text{infiltration}} = 0.03 \text{ L/s}$ ,  $\pm\sigma = 0 \text{ L/s}$ ), however we noted an increase of infiltration rate from JD232 (0.02 L/s) to JD238 (0.04 L/s). This increment might be explained by some detachments of some localized periphyton patches, and this was partly consistent with the slight increase in bed roughness (Figure 3a).

The infiltration rates of FA and FB did not show significant differences (Kruskal–Wallis:  $p > 0.05$ ) during the second phase of the experiment, thus suggesting that the introduction of disturbances had little influence on the infiltration of FA; although we found some

evidence of the impact of disturbances in FA. This was further demonstrated by the overall significant (Mann–Kendall:  $p < 0.05$ ) reduction in the infiltration rate, which dropped by  $\sim 76\%$  from JD196 (0.17 L/s) and JD249 (0.4 L/s) in FA and by  $\sim 84\%$  from JD196 (0.19 L/s) to JD249 (0.03 L/s) in FB. Our results suggested that the infiltration reduction related to the progressive filling of the interstices (FA: Pearson's correlation  $-0.58$ ,  $p < 0.01$ ; FB: Pearson's correlation  $-0.55$ ,  $p < 0.01$ ) and to the reduction of roughness (FA: Pearson's correlation 0.76,  $p < 0.01$ ; FB: Pearson's correlation 0.85,  $p < 0.01$ ).

### 3.3 | Hydraulics

Although the development of periphyton modified the roughness in both flumes, the evolution of the turbulent structures was somehow contrasting. In disagreement with our hypothesis (H2a), we did not find a significant (Mann–Kendall:  $p > 0.05$ ) reduction in the median percentage of ejection and sweep events in FA (Figure 4a) between JD195 and JD223, although we noted a slight reduction of  $\sim 3\%$  from JD197 (64%) to JD223 (62%) in their median occurrence. In contrast and in agreement with H2a, in FB (Figure 5a) we the median percentage of ejections and sweeps was significantly reduced (Mann–Kendall:

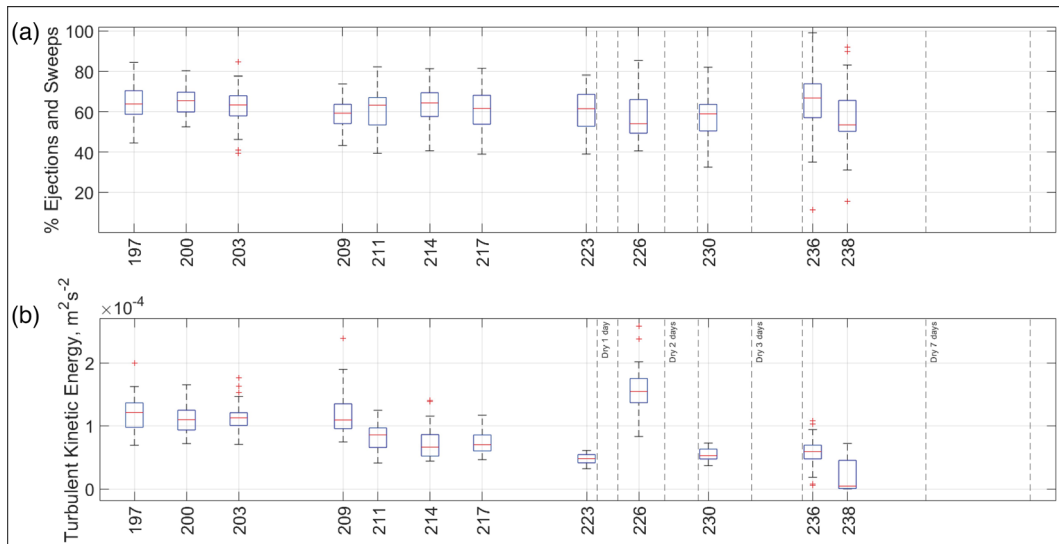


**FIGURE 4** FA hydraulics. (a) Percentage of ejection and sweep events at the near-bed layer. (b) Turbulent kinetic energy TKE ( $\text{m}^2\text{s}^{-2}$ ).

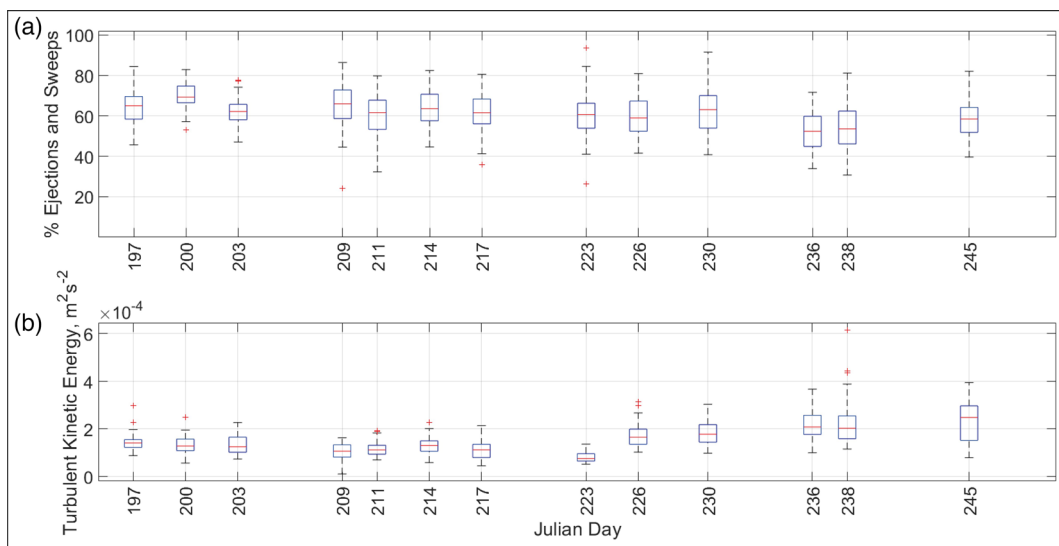


**FIGURE 5** FB hydraulics. (a) Percentage of ejection and sweep events at the near-bed layer. (b) Turbulent kinetic energy TKE ( $\text{m}^2\text{s}^{-2}$ ).

$p < 0.05$ ) by 6% (JD197: 65%; JD223: 61%). Surprisingly, we did not find significant differences (Kruskal–Wallis:  $p > 0.05$ ) in the median occurrence of ejections and sweeps between the flumes, suggesting a similar response of the near-bed layers and this regardless of the differences in decrease significance.

In agreement with H2a, our results suggested that the median TKE of FA (Figure 4b) was significantly (Mann–Kendall:  $p < 0.05$ ) reduced by  $\sim 61\%$  from JD197 ( $1.21 \times 10^{-4} \text{ m}^2\text{s}^{-2}$ ) to JD223 ( $4.78 \times 10^{-5} \text{ m}^2\text{s}^{-2}$ ). On the other hand and in disagreement with H2a, we did not find a significant (Mann–Kendall:  $p > 0.05$ ) negative trend in the median TKE for FB, although it dropped by  $\sim 47\%$  from JD197 ( $1.41 \times 10^{-4} \text{ m}^2\text{s}^{-2}$ ) to JD223 ( $7.53 \times 10^{-5} \text{ m}^2\text{s}^{-2}$ ). These dissimilarities were reflected in trends that were significantly different (Kruskal–Wallis:  $p < 0.05$ ), suggesting that the TKE evolved differently in the flumes, and this may have reflected differences in the periphyton morphologies.

The introduction of disturbances (from JD224 onwards) appeared to increase the occurrence of ejection and sweep events in FA

(Figure 4a), but only when desiccation was for longer than 1 day. In this sense, we noted an increase between JD226 (54%) and JD230 (59%) and one more important between JD230 and JD236 (66%). The latter resulted in a percentage of ejection and sweep events greater than at the beginning of the experiment. However, after the introduction of disturbances, and regardless of those localised increases, we did not find a significant upward trend (Mann–Kendall:  $p < 0.05$ ) in the occurrence of ejections and sweeps. Within this same period, the median percentage of ejection and sweep events in FB (Figure 5a) did not show significant (Mann–Kendall:  $p < 0.05$ ) increases or decreases, even though we reported a slight drop of 2%. Although we found evidence of localised impacts, the median occurrence of ejection and sweep events between the flumes did not differ significantly (Kruskal–Wallis:  $p > 0.05$ ) between the flumes, and this further suggested that the impact was only marginal as opposed to what we hypothesized (H2b).

Our results showed that the TKE of FA experienced an abrupt increase of  $\sim 222\%$  after the introduction of the first disturbance, that

is, between JD223 ( $4.78 \times 10^{-5} \text{ m}^2\text{s}^{-2}$ ) and JD226 ( $1.54 \times 10^{-4} \text{ m}^2\text{s}^{-2}$ ). This increase was followed by a slight decrease in ejection or sweep events (Figure 4a), hence an increase in inward or outward interactions. Then, our results did not suggest any other significant (Mann–Kendall:  $p > 0.05$ ) modification in the evolution of TKE. Within this same period, visual inspection of our results (Figure 5b) suggested an apparent increase in the median TKE of FB, which however was not found statistically significant (Mann–Kendall:  $p > 0.05$ ). The different evolutions in the median TKE were reflected in significant differences between the two trends (Kruskal–Wallis:  $p < 0.05$ ), identifying the potential role of disturbances in modifying the TKE of FA (H2b).

At the experiment timescale, we did not find a significant (Mann–Kendall:  $p > 0.05$ ) decrease of the median occurrence of ejections and sweeps in FA. However, the absence of a significant reduction must be contextualized. The drop was of  $\sim 17\%$  between JD197 (64%) and JD238 (53%), with a likelihood of being significant of 94% (Mann–Kendall:  $p = 0.06$ ) that leaves the possibility that the decrease had some significance for the processes being investigated here. In FB, the median occurrence of ejections and sweeps was significantly (Mann–Kendall:  $p < 0.05$ ) reduced by  $\sim 11\%$  from JD197 (65%) and JD245 (58%). Finally, the median TKE of FA was significantly (Mann–Kendall:  $p < 0.05$ ) reduced by  $\sim 96\%$  from JD197 ( $1.21 \times 10^{-4} \text{ m}^2\text{s}^{-2}$ ) to JD238 ( $4.60 \times 10^{-6} \text{ m}^2\text{s}^{-2}$ ), whereas the TKE of FB was significantly increased (Mann–Kendall:  $p < 0.05$ ) by  $\sim 76\%$  from JD197 ( $1.41 \times 10^{-4} \text{ m}^2\text{s}^{-2}$ ) to JD245 ( $2.48 \times 10^{-4} \text{ m}^2\text{s}^{-2}$ ).

## 4 | DISCUSSION

### 4.1 | Potential sources of errors

Flume experiments have been extensively used to investigate stream periphyton dynamics (e.g., Battin, Kaplan, Denis Newbold, & Hansen, 2003; Battin, Kaplan, Newbold, et al., 2003; Hondzo & Wang, 2002; Kazemifar et al., 2021; Mulholland et al., 1994; Nikora et al., 1997, 1998). Here, we decided to use photogrammetry to evaluate how the flume beds evolved in response to periphyton growth, and how this evolution modified the near-bed structures and the infiltration rate, primarily by modifying the surface roughness due to the biotic filling of the surficial interstices. Thus, it was necessary to acquire DEMs free of systematic and random errors (Butler et al., 1998; James et al., 2020) in order to provide reliable and accurate estimates of the changes in surface roughness. Different strategies have been proposed to do this. In this sense, a careful image acquisition design, a dense network of GCPs, and a good quality camera are expected in high-quality and high-precision photogrammetric studies (e.g., Butler et al., 2002; Chandler et al., 2001; James et al., 2017, 2020; Kasprak et al., 2015; Lane et al., 2001; Leduc et al., 2019; Morgan et al., 2017; O'Connor et al., 2017). In addition, when attempting to reconstruct submerged surfaces via photogrammetry the effect of refraction at the air–water interface must be corrected (Fryer & Kniest, 1985; Westaway et al., 2000, 2001), which is known to produce erroneous bed elevations and hence roughness underestimates (Butler et al., 2002).

Here, we used a good quality camera and a dense network of GCPs, but the use of standardized image acquisition geometries was

made impossible by the logistical complexity of our flume experiment, and the short windows of image capture (i.e., to ensure homogenous light conditions and avoid flume–wall related shadows). As such, our DEMs were impacted by both random and systematic errors. We successfully removed the systematic deformations, but some random errors still affected the quality of our DEMs although their magnitude was considered acceptable (see Supporting Information S1). We then corrected for the effect of refraction at the air–water interface, producing DEMs with low mean errors but with a tendency to inflate the random ones (see Supporting Information S1) presumably due to the undulation of the water surface.

Recognizing the potential presence of errors in DEMs is important in a study that attempts to analyse changes that can occur at millimetric scales. As we anticipated in Section 3.1, our estimates of the roughness, and particularly of the elevation lows, might have been impacted by such errors, leading to potential overestimates or underestimates of the parameters being analysed, and in turn in potentially inaccurate trend detection. Unfortunately, the data collected, processed, and presented here did not allow exploration of the sensitivity of our results to periphyton growth, and thus how these errors might have contributed to the overestimation or underestimation of the processes. That said, however, we argue that our results were coherent with the processes being investigated, and thus they captured them correctly in gross terms.

### 4.2 | Modification of the streambed and the near-bed hydraulics by periphyton

In this paper, we investigated how periphyton modify streambed properties and the near-bed hydraulics of tributary channels. We also attempted to understand if and how the introduction of disturbances in the form of short drying events (following Roncoroni et al., 2023) impacted the biogenic bed properties returning them to precolonization levels. We presented the results as follow: we analysed the evolution of the streambed and the near-bed hydraulics of both flumes before and after the introduction of disturbances in FA, but also at the experimental timescale (i.e., for the entire length of the experiment).

In the first part of the experiment (from JD195 to JD223), the periphyton development was very rapid in our flumes, and this had the consequence of modifying the beds (Figures 2 and 3). As expected (H1a), the roughness in both flumes was significantly reduced in this initial phase (Figures 2a and 3a). This finding agreed with some previous research (Fang et al., 2017; Godillot et al., 2001; Labiod et al., 2007), but disagreed with others (Nikora et al., 1997, 1998) who found rougher beds after the development of periphyton. The decreased in roughness was hypothesized to be related to the progressive filling of the surficial interstices (here referred as elevation lows), but in disagreement with H1a we did not find a significant filling in this first phase. However, visual inspection of our results (Figures 2b and 3b) suggested that the interstices were filled by biomass in the first 5 to 6 days. This is consistent with research in other environments (Cunningham et al., 1991), and the absence of a significant increase of the lows likely related to noise in our data.

The bed of FA, exposed to drying events from JD224 to JD249, was expected to return to levels of roughness and elevation lows

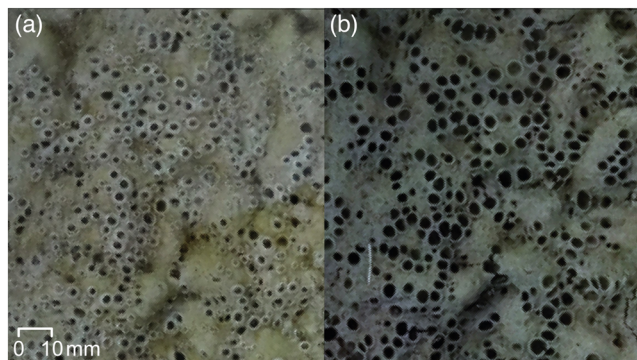


**FIGURE 6** (a) Periphyton active, producing air bubbles through photosynthesis in FA (JD223); (b) Periphyton mat just after water was removed (JD224).

similar to those prior to the colonization of periphyton after drying (H1b). Surprisingly, our results demonstrated that the roughness of FA did not return to a precolonized level suggesting that the bed morphology was likely preserved regardless of the wet-dry cycles. This finding was also supported by the absence of significant differences in the median roughness lengths between FA and FB. Indeed whilst FA was exposed to drying, both flumes experienced a phase of quasi-steadiness in which the roughness experienced low magnitude fluctuations. The latter were likely related to the detachment and regrowth of localized periphyton patches (see Figure 3d). However, we cannot exclude that these fluctuations were also a consequence of the buoyant nature of the periphyton due to the presence of air bubbles (Godillot et al., 2001; Labiod et al., 2007), and as suggested in Figure 6a. Similarly to roughness, the elevation lows of FA remained quasi-steady and did not return to levels similar to those of the start of the experiment on JD196, although we found significant differences in the lows of FA and FB. Thus, drying likely did not cause a return to preperiphyton conditions, but it did induce differences to conditions that remained inundated, related to changes in periphyton morphology, in differential noise, or to the introduction of disturbances in FA, and particularly to detachment of biomass in FA that occurred on JD238 (Figure 3b,d). The detachment likely originated following the 3-day dry conditions, and it was tracked as a sudden roughness increase, but we note that it was rapidly compensated thereafter.

At the experimental timescale (from JD195 to JD249), our results demonstrated that periphyton modified both flume beds, by reducing significantly the roughness and by raising significantly the lows (i.e., biomass filling). These findings further corroborated our initial hypothesis (H1a), even if the biomass that developed was markedly resilient and causing us to reject the hypotheses that disturbance would cause a return to preperiphyton conditions (H1b). Furthermore, these results demonstrated that although we were not able to find a significant increase in the lows of FA and FB during the initial phase (from JD195 to JD223), a significant increase was found by analysing the process at the experiment timescale. The filling likely happens over a long timescale and is associated with progressive biomass accumulation.

As we hypothesized (H3a), the infiltration of FA and FB was reduced significantly during the first part of the experiment (from JD195 to JD223), and the results reported here agreed with previous

work in terms of both process duration and infiltration rate (Cunningham et al., 1991; Orr et al., 2009; Ragusa et al., 1994). Following our results, it is clear that this reduction related to the clogging of the interstices, consistent with other studies (Battin & Sengschmitt, 1999; Caruso et al., 2017; Cunningham et al., 1991; Gette-Bouvarot et al., 2014; Ibsch & Borchardt, 2002; Orr et al., 2009; Thullner et al., 2002; Zhao et al., 2009). As with roughness and elevations lows, our hypothesis H3b was rejected since we did not find a significant difference between the infiltration of FA and FB when FA was subject to drying events. This suggested that the introduction of desiccation had little influence on the overall infiltration of FA, clearly because the biogenic bed preserved its morphology.

However, we noted that the infiltration rates in FA were typically and temporarily higher the day after the disturbance ended (+50% after 1 day, +33% after 2 days, 0% after 3 days, and +33% after 7 days), although this increase was suddenly followed by a new decrease. These patterns likely reflect the presence of millimetric holes in the mat surface of the dried periphyton mat that originated from escape of air bubbles encapsulated within the mat before the disturbance (Figure 6). Given that photosynthesis may stop during desiccation the associated holes likely lead to preferential infiltration paths. When inundation recommences, the sudden decrease in infiltration suggests that the organisms composing the mat survived desiccation and returned to being photosynthetically active. This happens at a timescale of only hours after re-submergence. This trend was found consistent with previous studies, notably in a similarly dry environment in Antarctica (Hawes & Howard-Williams, 1998; McKnight et al., 2007). It highlighted a concomitant process that we did not explore in this study. If the photosynthesis generated micro holes in the mat depend on the photosynthesis activity (i.e., light conditions vs dark conditions), it is possible that infiltration fluctuated daily, being lower when the periphyton continuously produced bubbles that filled the bubble-related micro holes (i.e., during the day time).

At the experimental timescale (from JD195 to JD249), the infiltration rates of FA and FB were both significantly reduced, by ~76% in FA and ~84% in FB, and this was related to the filling of the interstices and the decrease in surface roughness. At the experimental timescale, our hypothesis H3a that biofilm significantly reduce infiltration was confirmed for both flumes, but H3b was rejected because we could not find a significant impact of the dry-wet cycles. That said, however, the difference (8%) between the final infiltration rates may suggest that the disturbances produced a bed (FA) with a slightly lower capacity in retaining the water at the surface.

We hypothesized (H2a) that the decrease in bed roughness would have reduced the occurrence of ejections and sweeps and the turbulent kinetic energy (Figures 4 and 5). Although the roughness of both flumes was reduced (Figures 2a and 3a) in the first part of the experiment (JD195 to JD223), our results did not show a significant decrease in ejection and sweep events in FA, although we found a significant decrease in FB. In this initial phase, we reported a significant reduction of TKE in FA, but this was not found in FB.

We then hypothesized (H2b) that the introduction of disturbances (from JD224) would have changed the near-bed layer in response of the modification in surface roughness. We effectively found that desiccation events longer than 1 day resulted in an increase in ejections and sweeps. Surprisingly, such increases did not

match any real increase in bed roughness (Figure 2a) at least at the data resolution we obtained here. In addition, we did not find significant differences between the median percentage of sweeps and ejections of FA and FB, suggesting that the influence of disturbances was only marginal and punctual. In disagreement with H2b, the TKE of FA did not show a significant decrease or increase after the introduction of disturbances, but we noted an abrupt modification on JD226 (i.e., after the introduction of the first disturbance). The increase was of ~222%, and reflected in the ejection and sweep events being slightly decreased compared to JD223 and then again increased in JD230. This u-shaped trend between JD223 and JD230 might have suggested a more important contribution of inward and outward interactions on JD226, which are commonly the rarest events but which are recognized as being important as well (Nelson et al., 1995; Paiement-Paradis et al., 2011). This increase in TKE may have been related to a slight increase in roughness (Figure 2a) between JD224 (dry bed) and JD226 (re-submerged bed). Within this same period, the percentage of ejection and sweep events in FB was steady, which may reflect the fact that the roughness was also steady during the same period. As with FA, the TKE in FB did not show a significant increase or decrease, although visual inspection (Figure 5b) suggested an apparent increase.

A more interesting view of the modification of the near-bed layer was provided by its analysis at the experiment timescale. First, we found that the occurrence of ejections and sweeps in FB was significantly reduced by ~11% from JD197 to JD245. We did not find a significant decrease in FA at an alpha level of 0.05, but the reported *p* value (0.06) and the drop of ~17% between JD197 and JD238 likely suggested the presence of a negative trend, and therefore we might accept that ejection and sweep events were also decreased in FA. These findings agreed with our initial hypothesis (H2a) that the decrease in surface roughness would have reduced the occurrence of ejection and sweep events, as found by Reidenbach et al. (2010) and Kazemifar et al. (2021). This is relevant because sediment entrainment may be more likely in the presence of more ejections and sweeps (Bennett & Best, 1995; Dwivedi et al., 2011; Keylock et al., 2014), independently of changes in the shear stress (Shvidchenko & Pender, 2001). The findings highlighted therefore that periphyton led to beds less prone to ejection and sweep events that could entrain sediment particles, and this regardless of the introduction of disturbances (H2b).

Second, in disagreement with our initial hypothesis (H2a) but also with other research (Fang et al., 2017), we found that the TKE of FB tended to increase at the experiment timescale. This increase likely related to roughness and particularly to its fluctuations caused by cycles of detachment and regrowth of periphyton (i.e., increase or decrease in roughness) and the formation of holes and cracks in the mat (Figure 3d). The detachment processes occurred in conditions of stability (e.g., shear stress), and thus presumably related to episodes of self-detachment after the peak biomass was attained (Biggs, 1996) or because of the feeding activity of macrozoobenthos (Lamberti et al., 1987). In contrast, and in agreement with H2a, we found that the TKE of FA was significantly reduced from JD195 to JD238. Naturally, this finding was in disagreement with H2b that expected an increase in TKE after the introduction of disturbances. We could explain this tendency by the lower susceptibility to roughness fluctuations compared to FB (compare Figure 2a with Figure 3a), which in

turn could be explained by the lower probability of having biomass peak-related self-detachment events due to periodic desiccation events.

### 4.3 | Implications for ecosystem engineering

Periphyton development has been proposed as promoting primary succession in recently de-glaciated floodplains (Miller & Lane, 2019; Roncoroni et al., 2019). These authors hypothesized the formation of an impermeable layer at the sediment surface that reduced vertical infiltration of water, so maintaining standing water, and reduced susceptibility of sediment to erosion. Roncoroni et al. (2023) followed periphyton development over an entire melt season and showed that permanent periphyton development is limited to tributaries that flow over the most stable surfaces of glacial floodplains (i.e., terraces) due to high rates of stream erosion and deposition elsewhere but that it could also develop in secondary channels in the active zones of a braid plain, but where the high probability disturbance means this is rarely permanent. Terrace tributaries are commonly fed by snowmelt or ground water (Malard et al., 1999; Müller et al., 2022; Ward et al., 1999) and are substantially less harsh as compared to glacially fed channels (Boix Canadell et al., 2021). Our findings confirm that the Miller and Lane (2019) and Roncoroni et al. (2019) hypothesis that periphyton development can reduce infiltration does indeed hold. The speed with which it happens (Figures 2c and 3c) suggested that the onset of ecosystem engineering is extremely rapid. The experiments also show that the reduction in infiltration associated with periphyton development is not reset by wet-dry cycles. These changes have two major interrelated implications. First, periphyton development could be important in glacial floodplains as these are commonly well-drained with limited water retention (Burga et al., 2010; Cooper, 1923; Matthews, 1992; Viles, 2012). In theory this results in a more sustainable water supply to pioneer vegetation (Figure 7). Second, and however, the ecological engineering effect of periphyton in terms of infiltration is restricted to floodplain terraces as elsewhere disturbance rates are too high (Roncoroni et al., 2023). In the active braid plain, whilst periphyton can develop quickly in secondary channels where there is water, these rarely escape perturbation for long enough for primary plant colonization. Other zones within the active braidplain, further from secondary channels, are too dry to support periphyton development. The ecological engineering effect of periphyton-induced infiltration in terms of long-term vegetation succession following de-glaciation is then linked to a reduction in the intensity of fluvial reworking of the stream bed which destroys periphyton (Roncoroni et al., 2023).

It might be thought that biofilm and periphyton development could have a second ecosystem engineering effect via impacts on near-bed hydraulics, as has been shown for marine/tidal environments (Flemming & Wingender, 2010; Gerbersdorf & Wieprecht, 2015; Spears et al., 2008) and fine sediment fluvial environments (Schmidt et al., 2016; Thom et al., 2015). In the case studied here, we found that development of periphyton modifies the near-bed turbulent layer by reducing the occurrence of ejections and sweeps, so likely sediment entrainment. However, the effects are relatively small, and we hypothesize that in glacial environments it is likely insufficient to lead to significant biostabilization and reflected in the fact that periphyton

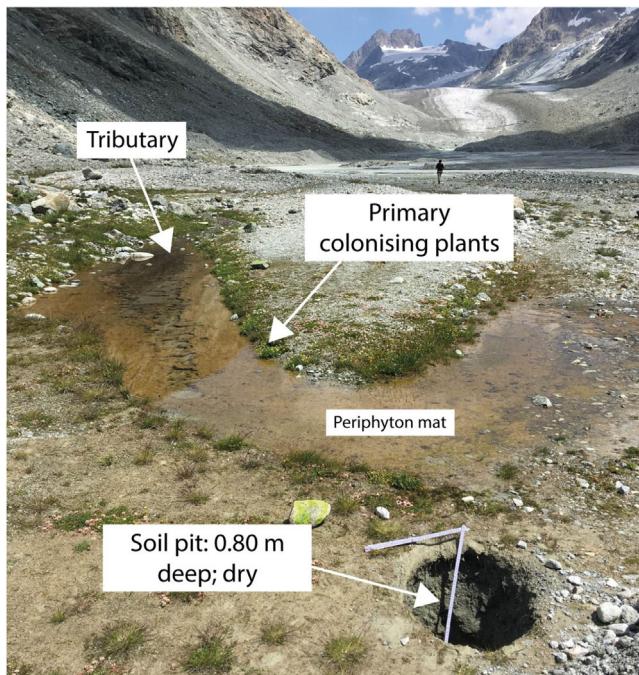


**FIGURE 7** Image of a tributary flowing across a terrace upstream of the flume experiments showing a periphyton mat retaining tributary derived water at the surface and encouraging local plant colonization.

survival in the active zone of braidplains is limited (Roncoroni et al., 2023). Periphyton have little effects on sediment entrainment per se in this environment, although they likely have important effects in reducing the detachment of periphyton patches. This may be a positive feedback by promoting infiltration rate reduction even if periphyton remain sensitive to morphodynamic induced disturbance.

## 5 | CONCLUSIONS

The modification of the streambed surface and hydraulic properties due to colonization of periphyton in proglacial margins was investigated with a set of outdoor flumes, and the combination of DEM and near-bed hydraulic analysis. We can draw the following main conclusions. First, the development of periphyton effectively filled the benthic interstices, and as a result reduced local bed roughness (H1a). Contrary to our hypothesis (H1b), the introduction of disturbances, here in the form of nonpermanent desiccation had limited effects on the biogenic bed, which preserved its predisturbance morphology. Second, the development of periphyton modified near-bed coherent structures. As hypothesized (H2a), the occurrence of ejection and sweep events was reduced, and this was particularly clear for the flume that was not disturbed by desiccation. Contrary to our hypothesis (H2b), the introduction of disturbances appeared to have little impact on the near-bed layer. Third, the filling of the sediment interstices clogged the streambed, and this had the result of reducing the rate at which water infiltrated into the sediment matrix (H3a). The introduction of disturbances might be expected to partly remove this feedback (H3b), but again our findings suggested that the desiccation events had only a little effect, with the undisturbed and disturbed flumes both maintaining low infiltration rates once periphyton had

developed throughout the full experiment. Thus, periphyton had a clear and distinctive ecological engineering effect through the reduction of infiltration and this was resilient to the desiccation events introduced here. This effect was realized after just a few days of inundation by clear water suggesting the effect was rapid. What limits the spatial extent to which this ecosystem engineering effect can drive vegetation succession is morphodynamic activity in the active braid plain. Therein, the zones with access to the water needed for periphyton development are also those where the risk of morphodynamic disturbance is greatest. This limits periphyton-driven vegetation succession in proglacial margins at least until morphodynamic reworking slows, likely related to changing glacier water and sediment supply.

Our experiments were a logistical challenge, and we recognized the possible sources of bias related to the complexity of running outdoor flume experiments in such an extreme environment (i.e., the forefield of an Alpine glacier at 2400 m a.s.l.). We also acknowledged that our findings may have reflected site-specific (e.g., water temperature and light conditions) and design-specific (e.g., grain size and flume slope) conditions that are difficult to replicate in other laboratory or outdoor studies. For these reasons, we call for new investigations that address the topic with different initial conditions and analytical approaches.

## ACKNOWLEDGEMENTS

We acknowledge the people that helped us in collecting the flume data during summer 2021, in no particular order: Frédéric Lardet, Antoine Guisolan, Alexandre Armada, and Anthony Félix. This study was supported by the Swiss National Science Foundation Sinergia grant awarded to T. I. Battin, S. N. Lane, M. Lever and P. Wilmes. Open access funding provided by Université de Lausanne.

## CONFLICT OF INTEREST STATEMENT

Stuart N. Lane is the Managing Editor of ESPL, but he was blinded from all elements of the review process which was managed by Professor M. J. Kirkby following journal policy.

## DATA AVAILABILITY STATEMENT

Flume DEMs are available at [zenodo.org/record/8058495](https://zenodo.org/record/8058495) and 3D flow velocities are available at [zenodo.org/record/8278434](https://zenodo.org/record/8278434).

## ORCID

Matteo Roncoroni  <https://orcid.org/0000-0001-6957-6225>

Stuart N. Lane  <https://orcid.org/0000-0002-6077-6076>

## REFERENCES

- Aberle, J. & Smart, G.M. (2003) The influence of roughness structure on flow resistance on steep slopes. *Journal of Hydraulic Research*, 41(3), 259–269. Available from: <https://doi.org/10.1080/00221680309499971>
- Amos, C.L., Bergamasco, A., Umgiesser, G., Cappucci, S., Cloutier, D., DeNat, L., et al. (2004) The stability of tidal flats in Venice Lagoon—the results of in-situ measurements using two benthic, annular flumes. *Journal of Marine Systems*, 51(1), 211–241. Available from: <https://doi.org/10.1016/j.jmarsys.2004.05.013>
- Bakker, M. & Lane, S.N. (2017) Archival photogrammetric analysis of river-floodplain systems using structure from motion (SfM) methods. *Earth Surface Processes and Landforms*, 42(8), 1274–1286. Available from: <https://doi.org/10.1002/esp.4085>

- Battin, T.J., Besemer, K., Bengtsson, M.M., Romani, A.M. & Packmann, A.I. (2016) The ecology and biogeochemistry of stream biofilms. *Nature Reviews Microbiology*, 14(4), 251–263. Available from: <https://doi.org/10.1038/nrmicro.2016.15>
- Battin, T.J., Kaplan, L.A., Denis Newbold, J. & Hansen, C.M.E. (2003) Contributions of microbial biofilms to ecosystem processes in stream mesocosms. *Nature*, 426(6965), 439–442. Available from: <https://doi.org/10.1038/nature02152>
- Battin, T.J., Kaplan, L.A., Newbold, J.D., Cheng, X. & Hansen, C. (2003) Effects of current velocity on the nascent architecture of stream microbial biofilms. *Applied and Environmental Microbiology*, 69(9), 5443–5452. Available from: <https://doi.org/10.1128/AEM.69.9.5443-5452.2003>
- Battin, T.J. & Sengschmitt, D. (1999) Linking sediment biofilms, hydrodynamics, and river bed clogging: evidence from a large river. *Microbial Ecology*, 37(3), 185–196. Available from: <https://doi.org/10.1007/s002489900142>
- Bennett, S.J. & Best, J.L. (1995) Mean flow and turbulence structure over fixed, two-dimensional dunes: implications for sediment transport and bedform stability. *Sedimentology*, 42(3), 491–513. Available from: <https://doi.org/10.1111/j.1365-3091.1995.tb00386.x>
- Bertin, S., Groom, J. & Friedrich, H. (2017) Isolating roughness scales of gravel-bed patches. *Water Resources Research*, 53(8), 6841–6856. Available from: <https://doi.org/10.1002/2016WR020205>
- Biggs, B.J.F. (1996) Patterns in benthic algae of streams. In: Stevenson, R.J., Bothwell, M.L. & Lowe, R.L. (Eds.) *Algal ecology: freshwater benthic ecosystems*, pp. 31–56. Available from: <https://doi.org/10.1016/B978-012668450-6/50031-X>
- Boix Canadell, M., Gómez-Gener, L., Ulseth, A.J., Cléménçon, M., Lane, S.N. & Battin, T.J. (2021) Regimes of primary production and their drivers in Alpine streams. *Freshwater Biology*, 66(8), 1449–1463. Available from: <https://doi.org/10.1111/fwb.13730>
- Breugem, W.P., Boersma, B.J. & Uittenbogaard, R.E. (2006) The influence of wall permeability on turbulent channel flow. *Journal of Fluid Mechanics*, 562, 35–72. Available from: <https://doi.org/10.1017/S0022112006000887>
- Burga, C.A., Krüsi, B., Egli, M., Wernli, M., Elsener, S., Ziefle, M., et al. (2010) Plant succession and soil development on the foreland of the Morteratsch glacier (Pontresina, Switzerland): straight forward or chaotic? *Flora - Morphology, Distribution, Functional Ecology of Plants*, 205(9), 561–576. Available from: <https://doi.org/10.1016/j.flora.2009.10.001>
- Butler, J., Lane, S., Chandler, J. & Porfiri, E. (2002) Through-water close range digital photogrammetry in flume and field environments. *The Photogrammetric Record*, 17(99), 419–439. Available from: <https://doi.org/10.1111/0031-868X.00196>
- Butler, J.B., Lane, S.N. & Chandler, J.H. (1998) Assessment of DEM quality for characterizing surface roughness using close range digital photogrammetry. *The Photogrammetric Record*, 16(92), 271–291. Available from: <https://doi.org/10.1111/0031-868X.00126>
- Caruso, A., Boano, F., Ridolfi, L., Chopp, D.L. & Packman, A. (2017) Biofilm-induced bioclogging produces sharp interfaces in hyporheic flow, redox conditions, and microbial community structure. *Geophysical Research Letters*, 44(10), 4917–4925. Available from: <https://doi.org/10.1002/2017GL073651>
- Cea, L., Puertas, J. & Pena, L. (2007) Velocity measurements on highly turbulent free surface flow using ADV. *Experiments in Fluids*, 42(3), 333–348. Available from: <https://doi.org/10.1007/s00348-006-0237-3>
- Chandler, J.H., Shiono, K., Rameshwaren, P. & Lane, S.N. (2001) Measuring flume surfaces for hydraulics research using a Kodak DCS460. *The Photogrammetric Record*, 17(97), 39–61. Available from: <https://doi.org/10.1111/0031-868X.00167>
- Cooper, W.S. (1923) The recent ecological history of Glacier Bay, Alaska: the present vegetation cycle. *Ecology*, 4(3), 223–246. Available from: <https://doi.org/10.2307/1929047>
- Cunningham, A.B., Characklis, W.G., Abedeen, F. & Crawford, D. (1991) Influence of biofilm accumulation on porous media hydrodynamics. *Environmental Science & Technology*, 25(7), 1305–1311. Available from: <https://doi.org/10.1021/es00019a013>
- Dade, W.B., Davis, J.D., Nichols, P.D., Nowell, A.R.M., Thistle, D., Trexler, M.B., et al. (1990) Effects of bacterial exopolymer adhesion on the entrainment of sand. *Geomicrobiology Journal*, 8(1), 1–16. Available from: <https://doi.org/10.1080/01490459009377874>
- Dwivedi, A., Melville, B.W., Shamseldin, A.Y. & Guha, T.K. (2011) Flow structures and hydrodynamic force during sediment entrainment. *Water Resources Research*, 47(1), 2010WR009089. Available from: <https://doi.org/10.1029/2010WR009089>
- Fang, H., Shang, Q., Chen, M. & He, G. (2014) Changes in the critical erosion velocity for sediment colonized by biofilm. *Sedimentology*, 61(3), 648–659. Available from: <https://doi.org/10.1111/sed.12065>
- Fang, H.W., Lai, H.J., Cheng, W., Huang, L. & He, G.J. (2017) Modeling sediment transport with an integrated view of the biofilm effects. *Water Resources Research*, 53(9), 7536–7557. Available from: <https://doi.org/10.1002/2017WR020628>
- Flemming, H.-C. & Wingender, J. (2010) The biofilm matrix. *Nature Reviews Microbiology*, 8(9), 623–633. Available from: <https://doi.org/10.1038/nrmicro2415>
- Fryer, J.G. & Kniest, H.T. (1985) Errors in depth determination caused by waves in through-water photogrammetry. *The Photogrammetric Record*, 11(66), 745–753. Available from: <https://doi.org/10.1111/j.1477-9730.1985.tb01326.x>
- Gerbersdorf, S.U., Jancke, T., Westrich, B. & Paterson, D.M. (2008) Microbial stabilization of riverine sediments by extracellular polymeric substances. *Geobiology*, 6(1), 57–69. Available from: <https://doi.org/10.1111/j.1472-4669.2007.00120.x>
- Gerbersdorf, S.U., Manz, W. & Paterson, D.M. (2008) The engineering potential of natural benthic bacterial assemblages in terms of the erosion resistance of sediments. *FEMS Microbiology Ecology*, 66(2), 282–294. Available from: <https://doi.org/10.1111/j.1574-6941.2008.00586.x>
- Gerbersdorf, S.U., Westrich, B. & Paterson, D.M. (2009) Microbial extracellular polymeric substances (EPS) in fresh water sediments. *Microbial Ecology*, 58, 334–349. Available from: <https://doi.org/10.1007/s00248-009-9498-8>
- Gerbersdorf, S.U. & Wiprecht, S. (2015) Biostabilization of cohesive sediments: revisiting the role of abiotic conditions, physiology and diversity of microbes, polymeric secretion, and biofilm architecture. *Geobiology*, 13(1), 68–97. Available from: <https://doi.org/10.1111/gbi.12115>
- Gette-Bouvarot, M., Mermillod-Blondin, F., Angulo-Jaramillo, R., Delolme, C., Lemoine, D., Lassabatere, L., et al. (2014) Coupling hydraulic and biological measurements highlights the key influence of algal biofilm on infiltration basin performance. *Ecohydrology*, 7(3), 950–964. Available from: <https://doi.org/10.1002/eco.1421>
- Godillot, R., Caussade, B., Ameziane, T. & Capblancq, J. (2001) Interplay between turbulence and periphyton in rough open-channel flow. *Journal of Hydraulic Research*, 39(3), 227–239. Available from: <https://doi.org/10.1080/00221680109499826>
- Goring, D.G. & Nikora, V.I. (2002) Despiking acoustic doppler velocimeter data. *Journal of Hydraulic Engineering*, 128(1), 117–126. Available from: [https://doi.org/10.1061/\(ASCE\)0733-9429\(2002\)128:1\(117\)](https://doi.org/10.1061/(ASCE)0733-9429(2002)128:1(117))
- Grant, J. & Gust, G. (1987) Prediction of coastal sediment stability from photopigment content of mats of purple sulphur bacteria. *Nature*, 330(6145), 244–246. Available from: <https://doi.org/10.1038/330244a0>
- Hawes, I. & Howard-Williams, C. (1998) Primary production processes in streams of the Mcmurdo Dry Valleys, Antarctica. In: Priscu, J.C. (Ed.) *Ecosystem dynamics in a polar desert: the Mcmurdo Dry Valleys, Antarctica*. American Geophysical Union (AGU), pp. 129–140 <https://doi.org/10.1029/AR072p0129>
- Hondzo, M. & Wang, H. (2002) Effects of turbulence on growth and metabolism of periphyton in a laboratory flume. *Water Resources Research*, 38(12), 13-1–13-19. Available from: <https://doi.org/10.1029/2002WR001409>
- Ibisch, R.B. & Borchardt, D. (2002) Effects of periphyton biomass and suspended solids on river bed permeability and hyporheic oxygen balances. *SIL Proceedings*, 1922–2010, 28(4), 1875–1879. Available from: <https://doi.org/10.1080/03680770.2001.11901954>

- James, M.R., Antoniazza, G., Robson, S. & Lane, S.N. (2020) Mitigating systematic error in topographic models for geomorphic change detection: accuracy, precision and considerations beyond off-nadir imagery. *Earth Surface Processes and Landforms*, 45(10), 2251–2271. Available from: <https://doi.org/10.1002/esp.4878>
- James, M.R. & Robson, S. (2014) Mitigating systematic error in topographic models derived from UAV and ground-based image networks. *Earth Surface Processes and Landforms*, 39(10), 1413–1420. Available from: <https://doi.org/10.1002/esp.3609>
- James, M.R., Robson, S., d'Oleire-Oltmanns, S. & Niethammer, U. (2017) Optimising UAV topographic surveys processed with structure-from-motion: ground control quality, quantity and bundle adjustment. *Geomorphology*, 280, 51–66. Available from: <https://doi.org/10.1016/j.geomorph.2016.11.021>
- Kasprak, A., Wheaton, J.M., Ashmore, P.E., Hensleigh, J.W. & Peirce, S. (2015) The relationship between particle travel distance and channel morphology: results from physical models of braided rivers. *Journal of Geophysical Research - Earth Surface*, 120(1), 55–74. Available from: <https://doi.org/10.1002/2014JF003310>
- Kazemifar, F., Blois, G., Aybar, M., Perez Calleja, P., Nerenberg, R., Sinha, S., et al. (2021) The effect of biofilms on turbulent flow over permeable beds. *Water Resources Research*, 57(2), e2019WR026032. Available from: <https://doi.org/10.1029/2019WR026032>
- Keylock, C.J., Lane, S.N. & Richards, K.S. (2014) Quadrant/octant sequencing and the role of coherent structures in bed load sediment entrainment. *Journal of Geophysical Research - Earth Surface*, 119(2), 264–286. Available from: <https://doi.org/10.1002/2012JF002698>
- Labioud, C., Godillot, R. & Caussade, B. (2007) The relationship between stream periphyton dynamics and near-bed turbulence in rough open-channel flow. *Ecological Modelling*, 209(2), 78–96. Available from: <https://doi.org/10.1016/j.ecolmodel.2007.06.011>
- Lamberti, G.A., Ashkenas, L.R., Gregory, S.V. & Steinman, A.D. (1987) Effects of three herbivores on periphyton communities in laboratory streams. *Journal of the North American Benthological Society*, 6(2), 92–104. Available from: <https://doi.org/10.2307/1467219>
- Lane, S.N., Chandler, J.H. & Porfiri, K. (2001) Monitoring river channel and flume surfaces with digital photogrammetry. *Journal of Hydraulic Engineering*, 127(10), 871–877. Available from: [https://doi.org/10.1061/\(ASCE\)0733-9429\(2001\)127:10\(871\)](https://doi.org/10.1061/(ASCE)0733-9429(2001)127:10(871))
- Le Hir, P., Monbet, Y. & Orvain, F. (2007) Sediment erodability in sediment transport modelling: can we account for biota effects? *Continental Shelf Research*, 27(8), 1116–1142. Available from: <https://doi.org/10.1016/j.csr.2005.11.016>
- Leduc, P., Peirce, S. & Ashmore, P. (2019) Short communication: challenges and applications of structure-from-motion photogrammetry in a physical model of a braided river. *Earth Surface Dynamics*, 7(1), 97–106. Available from: <https://doi.org/10.5194/esurf-7-97-2019>
- Malard, F., Tockner, K. & Ward, J.V. (1999) Shifting dominance of sub-catchment water sources and flow paths in a glacial floodplain, Val Roseg, Switzerland. *Arctic, Antarctic, and Alpine Research*, 31(2), 135–150. Available from: <https://doi.org/10.1080/15230430.1999.12003291>
- Mancini, D. & Lane, S.N. (2020) Changes in sediment connectivity following glacial debuiting in an Alpine valley system. *Geomorphology*, 352, 106987. Available from: <https://doi.org/10.1016/j.geomorph.2019.106987>
- Mariotti, G. & Fagherazzi, S. (2012) Modeling the effect of tides and waves on benthic biofilms. *Journal of Geophysical Research - Biogeosciences*, 117(G4), 2012JG002064. Available from: <https://doi.org/10.1029/2012JG002064>
- Matthews, J.A. (1992) *The ecology of recently-deglaciated terrain: a geoecological approach to glacier forelands*. Cambridge: Cambridge University Press.
- McKnight, D.M., Tate, C.M., Andrews, E.D., Niyogi, D.K., Cozzetto, K., Welch, K., et al. (2007) Reactivation of a cryptobiotic stream ecosystem in the McMurdo Dry Valleys, Antarctica: a long-term geomorphological experiment. *Geomorphology*, 89(1–2), 186–204. Available from: <https://doi.org/10.1016/j.geomorph.2006.07.025>
- Mianaei, S.J. & Keshavarzi, A.R. (2010) Study of near bed stochastic turbulence and sediment entrainment over the ripples at the bed of open channel using image processing technique. *Stochastic Environmental Research and Risk Assessment*, 24(5), 591–598. Available from: <https://doi.org/10.1007/s00477-009-0346-7>
- Miller, H.R. & Lane, S.N. (2019) Biogeomorphic feedbacks and the ecosystem engineering of recently deglaciated terrain. *Progress in Physical Geography: Earth and Environment*, 43(1), 24–45. Available from: <https://doi.org/10.1177/0309133318816536>
- Morgan, J.A., Brogan, D.J. & Nelson, P.A. (2017) Application of structure-from-motion photogrammetry in laboratory flumes. *Geomorphology*, 276, 125–143. Available from: <https://doi.org/10.1016/j.geomorph.2016.10.021>
- Mulholland, P.J., Steinman, A.D., Marzolf, E.R., Hart, D.R. & DeAngelis, D.L. (1994) Effect of periphyton biomass on hydraulic characteristics and nutrient cycling in streams. *Oecologia*, 98(1), 40–47. Available from: <https://doi.org/10.1007/BF00326088>
- Müller, T., Lane, S.N. & Schaeffli, B. (2022) Towards a hydrogeomorphological understanding of proglacial catchments: an assessment of groundwater storage and release in an Alpine catchment. *Hydrology and Earth System Sciences*, 26(23), 6029–6054. Available from: <https://doi.org/10.5194/hess-26-6029-2022>
- Nelson, J.M., Shreve, R.L., McLean, S.R. & Drake, T.G. (1995) Role of near-bed turbulence structure in bed load transport and bed form mechanics. *Water Resources Research*, 31(8), 2071–2086. Available from: <https://doi.org/10.1029/95WR00976>
- Neumeier, U., Lucas, C.H. & Collins, M. (2006) Erodibility and erosion patterns of mudflat sediments investigated using an annular flume. *Aquatic Ecology*, 40(4), 543–554. Available from: <https://doi.org/10.1007/s10452-004-0189-8>
- Nezu, I. & Nakagawa, H. (1993). *Turbulence in open channel flows*. Rotterdam, Netherlands: IAHR Monograph, Balkema.
- Nikora, V.I. & Goring, D.G. (1998) ADV measurements of turbulence: can we improve their interpretation? *Journal of Hydraulic Engineering*, 124(6), 630–634. Available from: [https://doi.org/10.1061/\(ASCE\)0733-9429\(1998\)124:6\(630\)](https://doi.org/10.1061/(ASCE)0733-9429(1998)124:6(630))
- Nikora, V.I., Goring, D.G. & Biggs, B.J.F. (1997) On stream periphyton-turbulence interactions. *New Zealand Journal of Marine and Freshwater Research*, 31(4), 435–448. Available from: <https://doi.org/10.1080/00288330.1997.9516777>
- Nikora, V.I., Goring, D.G. & Biggs, B.J.F. (1998) A simple model of stream periphyton-flow interactions. *Oikos*, 81(3), 607. Available from: <https://doi.org/10.2307/3546782>
- Nikora, V.I., Goring, D.G. & Biggs, B.J.F. (2002) Some observations of the effects of micro-organisms growing on the bed of an open channel on the turbulence properties. *Journal of Fluid Mechanics*, 450, 317–341. Available from: <https://doi.org/10.1017/S0022112001006486>
- O'Connor, J., Smith, M.J. & James, M.R. (2017) Cameras and settings for aerial surveys in the geosciences: optimising image data. *Progress in Physical Geography: Earth and Environment*, 41(3), 325–344. Available from: <https://doi.org/10.1177/0309133317703092>
- Orr, C.H., Clark, J.J., Wilcock, P.R., Finlay, J.C. & Doyle, M.W. (2009) Comparison of morphological and biological control of exchange with transient storage zones in a field-scale flume. *Journal of Geophysical Research - Biogeosciences*, 114(G2), 2008JG000825. Available from: <https://doi.org/10.1029/2008JG000825>
- Paiement-Paradis, G., Marquis, G. & Roy, A. (2011) Effects of turbulence on the transport of individual particles as bedload in a gravel-bed river. *Earth Surface Processes and Landforms*, 36(1), 107–116. Available from: <https://doi.org/10.1002/esp.2027>
- Piqué, G., Vericat, D., Sabater, S. & Batalla, R.J. (2016) Effects of biofilm on river-bed scour. *Science of the Total Environment*, 572, 1033–1046. Available from: <https://doi.org/10.1016/j.scitotenv.2016.08.009>
- Pivato, M., Carniello, L., Moro, I. & D'Odorico, P. (2019) On the feedback between water turbidity and microphytobenthos growth in shallow tidal environments. *Earth Surface Processes and Landforms*, 44(5), 1192–1206. Available from: <https://doi.org/10.1002/esp.4567>
- Ragusa, S.R., de Zoysa, D.S. & Rengasamy, P. (1994) The effect of microorganisms, salinity and turbidity on hydraulic conductivity of irrigation channel soil. *Irrigation Science*, 15(4), 159–166. Available from: <https://doi.org/10.1007/BF00193683>

- Reidenbach, M.A., Limm, M., Hondzo, M. & Stacey, M.T. (2010) Effects of bed roughness on boundary layer mixing and mass flux across the sediment-water interface. *Water Resources Research*, 46(7), 2009WR008248. Available from: <https://doi.org/10.1029/2009WR008248>
- Roncoroni, M., Brandani, J., Battin, T.I. & Lane, S.N. (2019) Ecosystem engineers: biofilms and the ontogeny of glacier floodplain ecosystems. *Wiley Interdisciplinary Reviews Water*, 6(6), e1390. Available from: <https://doi.org/10.1002/wat2.1390>
- Roncoroni, M., Mancini, D., Miesen, F., Müller, T., Gianini, M., Ouvry, B., et al. (2023) Decrypting the stream periphyton physical habitat of recently deglaciated floodplains. *Science of the Total Environment*, 867, 161374. Available from: <https://doi.org/10.1016/j.scitotenv.2022.161374>
- Schmidt, H., Thom, M., King, L., Wieprecht, S. & Gerbersdorf, S.U. (2016) The effect of seasonality upon the development of lotic biofilms and microbial biostabilisation. *Freshwater Biology*, 61(6), 963–978. Available from: <https://doi.org/10.1111/fwb.12760>
- Shvidchenko, A.B. & Pender, G. (2001) Macroturbulent structure of open-channel flow over gravel beds. *Water Resources Research*, 37(3), 709–719. Available from: <https://doi.org/10.1029/2000WR900280>
- Smart, G., Aberle, J., Duncan, M. & Walsh, J. (2004) Measurement and analysis of alluvial bed roughness. *Journal of Hydraulic Research*, 42(3), 227–237. Available from: <https://doi.org/10.1080/00221686.2004.9728388>
- Spears, B.M., Saunders, J.E., Davidson, I. & Paterson, D.M. (2008) Microalgal sediment biostabilisation along a salinity gradient in the Eden Estuary, Scotland: unravelling a paradox. *Marine and Freshwater Research*, 59(4), 313–321. Available from: <https://doi.org/10.1071/MF07164>
- Statzner, B., Arens, M.-F., Champagne, J.-Y., Morel, R. & Herouin, E. (1999) Silk-producing stream insects and gravel erosion: significant biological effects on critical shear stress. *Water Resources Research*, 35(11), 3495–3506. Available from: <https://doi.org/10.1029/1999WR900196>
- Suga, K., Matsumura, Y., Ashitaka, Y., Tominaga, S. & Kaneda, M. (2010) Effects of wall permeability on turbulence. *International Journal of Heat and Fluid Flow*, 31(6), 974–984. Available from: <https://doi.org/10.1016/j.ijheatfluidflow.2010.02.023>
- Thom, M., Schmidt, H., Gerbersdorf, S.U. & Wieprecht, S. (2015) Seasonal biostabilization and erosion behavior of fluvial biofilms under different hydrodynamic and light conditions. *International Journal of Sediment Research*, 30(4), 273–284. Available from: <https://doi.org/10.1016/j.ijsrc.2015.03.015>
- Thomas, R.E., Schindfessel, L., McLelland, S.J., Creëlle, S. & Mulder, T.D. (2017) Bias in mean velocities and noise in variances and covariances measured using a multistatic acoustic profiler: the Nortek Vectrino Profiler. *Measurement Science and Technology*, 28(7), 075302. Available from: <https://doi.org/10.1088/1361-6501/aa7273>
- Thorne, P.D., Williams, J.J. & Heathershaw, A.D. (1989) In situ acoustic measurements of marine gravel threshold and transport. *Sedimentology*, 36(1), 61–74. Available from: <https://doi.org/10.1111/j.1365-3091.1989.tb00820.x>
- Thullner, M., Zeyer, J. & Kinzelbach, W. (2002) Influence of microbial growth on hydraulic properties of pore networks. *Transport in Porous Media*, 49(1), 99–122. Available from: <https://doi.org/10.1023/A:1016030112089>
- Tolhurst, T.J., Gust, G. & Paterson, D.M. (2002) The influence of an extracellular polymeric substance (EPS) on cohesive sediment stability. *Proceedings in Marine Science*, 5, 409–425. [https://doi.org/10.1016/S1568-2692\(02\)80030-4](https://doi.org/10.1016/S1568-2692(02)80030-4)
- Vignaga, E., Sloan, D.M., Luo, X., Haynes, H., Phoenix, V.R. & Sloan, W.T. (2013) Erosion of biofilm-bound fluvial sediments. *Nature Geoscience*, 6(9), 770–774. Available from: <https://doi.org/10.1038/ngeo1891>
- Viles, H.A. (2012) Microbial geomorphology: a neglected link between life and landscape. *Geomorphology*, 157–158, 6–16. Available from: <https://doi.org/10.1016/j.geomorph.2011.03.021>
- Ward, J.V., Malard, F., Tockner, K. & Uehlinger, U. (1999) Influence of ground water on surface water conditions in a glacial flood plain of the Swiss Alps. *Hydrological Processes*, 13(3), 277–293. Available from: [https://doi.org/10.1002/\(SICI\)1099-1085\(19990228\)13:3<277::AID-HYP738>3.0.CO;2-N](https://doi.org/10.1002/(SICI)1099-1085(19990228)13:3<277::AID-HYP738>3.0.CO;2-N)
- Westaway, R.M., Lane, S.N. & Hicks, D.M. (2000) The development of an automated correction procedure for digital photogrammetry for the study of wide, shallow, gravel-bed rivers. *Earth Surface Processes and Landforms*, 25(2), 209–226. Available from: [https://doi.org/10.1002/\(SICI\)1096-9837\(200002\)25:2%3C209::AID-ESP84%3E3.0.CO;2-Z](https://doi.org/10.1002/(SICI)1096-9837(200002)25:2%3C209::AID-ESP84%3E3.0.CO;2-Z)
- Westaway, R.M., Lane, S.N. & Hicks, D.M. (2001) Remote sensing of clear-water, shallow, gravel-bed rivers using digital photogrammetry. *Photogrammetric Engineering and Remote Sensing*, 67, 1271–1282.
- Westoby, M.J., Brasington, J., Glasser, N.F., Hambrey, M.J. & Reynolds, J.M. (2012) ‘Structure-from-motion’ photogrammetry: a low-cost, effective tool for geoscience applications. *Geomorphology*, 179, 300–314. Available from: <https://doi.org/10.1016/j.geomorph.2012.08.021>
- Widdows, J., Brinsley, M.D., Salkeld, P.N. & Lucas, C.H. (2000) Influence of biota on spatial and temporal variation in sediment erodability and material flux on a tidal flat (Westerschelde, The Netherlands). *Marine Ecology Progress Series*, 194, 23–37. Available from: <https://doi.org/10.3354/meps194023>
- Wu, F.-C. & Jiang, M.-R. (2007) Numerical investigation of the role of turbulent bursting in sediment entrainment. *Journal of Hydraulic Engineering*, 133(3), 329–334. Available from: [https://doi.org/10.1061/\(ASCE\)0733-9429\(2007\)133:3\(329\)](https://doi.org/10.1061/(ASCE)0733-9429(2007)133:3(329))
- Zhao, L., Zhu, W. & Tong, W. (2009) Clogging processes caused by biofilm growth and organic particle accumulation in lab-scale vertical flow constructed wetlands. *Journal of Environmental Sciences*, 21(6), 750–757. Available from: [https://doi.org/10.1016/S1001-0742\(08\)62336-0](https://doi.org/10.1016/S1001-0742(08)62336-0)

## SUPPORTING INFORMATION

Additional supporting information can be found online in the Supporting Information section at the end of this article.

**How to cite this article:** Roncoroni, M., Ballu, A., Selitaj, A., Mancini, D., Miesen, F., Aguet, M. et al. (2023) Ecosystem engineering by periphyton in Alpine proglacial streams. *Earth Surface Processes and Landforms*, 1–15. Available from: <https://doi.org/10.1002/esp.5712>